Modulation of the extraordinary optical transmission by surface acoustic waves

Davy Gérard,[*] Vincent Laude, Benattou Sadani, Abdelkrim Khelif, Daniel Van Labeke, and Brahim Guizal

Institut FEMTO-ST, UMR CNRS 6174, Université de Franche-Comté, 32 Avenue de l'observatoire, F-25044 Besançon Cedex, France

The numerical study of the acoustic (elastic) effect in periodically nanostructured metallic films exhibiting extraordinary optical transmission (EOT) deposited onto the top of a piezoelectric material is reported. Surface acoustic waves are generated in the piezoelectric substrate and their influence in the transmission spectrum of the EOT structure is studied. It is shown that low frequency acoustic waves can significantly tune the resonance frequency of the EOT structure and modulate the transmitted intensity. Acoustic waves appear as an interesting route to realize controllable EOT devices and other active plasmonic components.

I. INTRODUCTION

Nanostructured metallic films, such as arrays of subwavelength holes or slits,[1,2] single apertures surrounded by a corrugation,[3] or continuous films presenting a periodical texturing of their surface,[4] exhibit remarkable optical properties. One of these properties is the so-called "extraordinary optical transmission" (EOT): an array of subwavelength apertures exhibits resonances in its transmission spectrum where the transmission efficiency is significantly higher than one would expect by simply considering the surface occupied by the apertures. The EOT phenomenon has mainly two origins: electromagnetic surface modes at the surface of the metal (surface plasmons) and guided modes inside the apertures (when apertures exist). Another remarkable property of nanostructured metallic films is the presence of high amplitude electromagnetic fields both at the surface and inside the apertures. This is why these structures are promising for a wide range of applications, such as surface enhanced Raman scattering, angle-independent filtering,[5] enhancement of nonlinear properties,[6,7] enhancement of single molecule fluorescence,[8] biosensing,[9] or polarization of light at the nanoscale.[10] Recent reviews of this topic can be found in Ref. 11 and 12. However, for actual applications, it is desirable to control the optical properties of nanostructures by an external signal. All-optical control (through a third order nonlinearity) of the transmission through an array of apertures has been previously reported.[13] However, this study evidenced on and/or off switching of the EOT, not continuous modulation.

In this paper, we focus our attention on the control of EOT by using surface acoustic waves (SAWs) generated in a piezoelectric material. SAWs are usually generated by interdigital transducers (IDTs), consisting of a periodical array of metallic stripes (electrodes). The period of the stripes, which is related to the wavelength of the acoustic waves, is typically 500 nm for a SAW frequency of 3 GHz in a material such as lithium niobate (LiNbO$_3$). Such dimensions are well suited for EOT in the visible and near-infrared region. Therefore, one can imagine a device consisting of a metallic grating deposited on a piezoelectric substrate: it would exhibit EOT properties, and its optical transmission would be tunable by using the same metallic grating as a piezoelectric transducer. In the following, we will discuss the feasibility of such a device by exploring different geometries with numerical experiments. We will show that, indeed, the ideal geometry discussed above (where the EOT structure acts also as an IDT) is unfortunately not appropriate and we will propose a more efficient design. To account for acousto-optical interactions, we use a simple numerical approach in two steps. Rather than using some "multiphysics" algorithm, we first estimate the acousto-optic effect with one algorithm, and then enter data from the acoustic code in our electromagnetic solver.

The paper is organized as follows. In Sec. II, we present the EOT structure, without considering any acousto-optic interaction. The structure is a one-dimensional metallic grating deposited on the top of a lithium niobate substrate, and it exhibits a high amplitude transmission resonance. Section III is devoted to the study of the acousto-optic interaction in the nanostructured metallic film, in the case where the metallic grating acts as a piezoelectric transducer. In Sec. IV, we present another design, where a long wavelength SAW changes globally the refractive index of the substrate. We show that this approach can lead to significant tunability of the transmission resonance, providing that the elasto-optic effect is strong enough. Finally, in Sec. V, we summarize our results and draw some perspectives.

II. EXTRAORDINARY TRANSMISSION THROUGH A ONE-DIMENSIONAL METALLIC GRATING ON LITHIUM NIOBATE

The structure under consideration is schematically drawn in Fig. 1. It consists of a one-dimensional gold grating deposited onto a semi-infinite *Y*-cut LiNbO$_3$ substrate. The
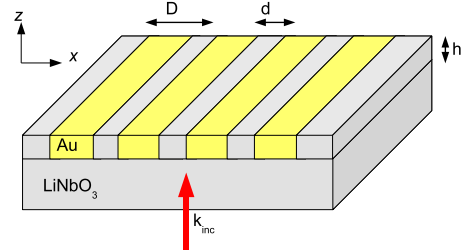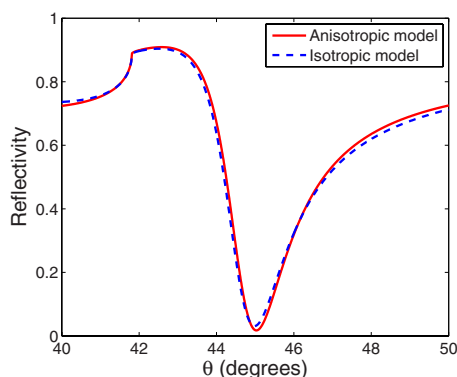

FIG. 1. (Color online) Sketch of the EOT structure.

FIG. 2. (Color online) Computed reflectivity of a gold film deposited on a prism, in a attenuated total reflection setup. Solid line: the anisotropic dielectric tensor is taken into account. Dashed line: the substrate is approximated by an isotropic layer.

structure is assumed to be infinite in the y direction, and to be periodic in the x direction. The y axis is aligned with the Z crystallographic axis. The slits of the grating (i.e., the space between each metallic stripe) are filled with $LiNbO_3$. The period of the grating is D, the width of the slits is d, and the gold film thickness is set to h. The dielectric permittivity of gold is taken from tabulated experimental data.[14] The grating is illuminated under normal incidence from the substrate side by a monochromatic, p-polarized (electric field perpendicular to the direction of invariance of the slits) plane wave.

The most important assumption we made in the computations is that the substrate is optically isotropic. Strictly speaking, this assumption is obviously wrong since $LiNbO_3$ is an anisotropic (uniaxial) material. In order to check the role played by the anisotropy of the substrate, we have made numerical simulations of an uniform gold film deposited on a 1 μm thick Y-cut $LiNbO_3$ layer, this layer being deposited onto the top of a semi-infinite glass substrate. To compute the reflection efficiency through the layered structure, a T-matrix method has been employed.[15] Figure 2 reports the reflectivity as a function of the angle of incidence, first considering the substrate as an isotropic material (with a refractive index set to the average value between the ordinary index and the extraordinary index) and second by taking into account the anisotropy of the dielectric permittivity. In each case, a strong dip of reflectivity appears on the spectrum, associated with the excitation of a surface plasmon on the gold/air interface. Comparison between the isotropic and anisotropic cases shows that the anisotropy does not influence much the plasmon resonance. The position of the reflectivity minimum is shifted by less than 0.05° and the resonance width is the same. It should be stressed that the plasmon resonance of an interface is extremely sensitive to small variations in the refractive indices of the neighboring media. This is a strong indication that the optical properties of our metallic grating (mostly governed by plasmon resonances and guided modes inside the apertures) will not be affected much by the anisotropy of the substrate. A similar behavior has been observed experimentally by Sun *et al.*[16] As a consequence, in all the following calculations, the lithium niobate substrate is assumed to be an optically isotropic and non dispersive material, its dielectric permittivity being set to $\varepsilon = 5.05$.
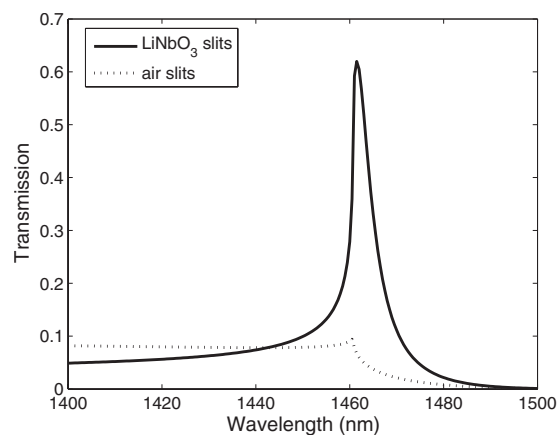

FIG. 3. Transmission spectrum through a grating with $D = 650$ nm, $d = 100$ nm, and $h = 90$ nm, when the slits are filled with lithium niobate (solid line) and when the slits are filled with air (dotted line).

All electromagnetic calculations presented below were made using the Fourier modal method equipped with the S-matrix algorithm to prevent instabilities[17] and the correct rules of Fourier factorization to improve convergence.[18,19] Figure 3, solid line, plots the zeroth order transmission through a structure with period $D = 650$ nm, slit width $d = 100$ nm, and thickness $h = 90$ nm. A high amplitude transmission resonance is observed, with a reasonably good quality factor. The width of the resonance is in striking contrast with the low quality factor that is generally linked to the high transmittance peaks of slits gratings.[2] Generally speaking, EOT structures presenting a good transmittance (like annular apertures arrays[20]) rely on guided modes, but the drawback is that this high transmittance is associated with relatively broad resonance peaks. In contrast, here we obtain a transmission resonance combining good transmission and a quite good quality factor. We attribute this resonance to the coupling between a surface plasmon propagating along the gold/$LiNbO_3$ interface and an evanescent mode inside the slits. This assumption is well supported by the following facts: (i) if the slits are filled with air rather than $LiNbO_3$, then the resonance is destroyed (see Fig. 3, dotted line) because of the impedance mismatch between the surface plasmon and the guided mode at the entrance of the slit. (ii) The position of the resonance is given approximately by the product of the refractive index of the substrate times the period, indicating a surface plasmon excitation at the metal/substrate interface. This property of the resonance will be exploited in Sec. IV. (iii) The near-field map at resonance (see Fig. 4) evidences a high optical intensity both at the metal surface and inside the slits. This also suggests the presence of both a surface wave (horizontal resonance) and a guided mode (vertical resonance).[21] The hybrid nature of the resonance is interesting for the applications we are looking at since it implies that the resonance frequency may be controlled either by tuning the guided mode or the surface mode.

III. ACOUSTO-OPTIC INTERACTION IN A NANOSTRUCTURED METALLIC FILM

From now on, we consider that a SAW (Rayleigh wave) is propagating along the surface of the piezoelectric substrate
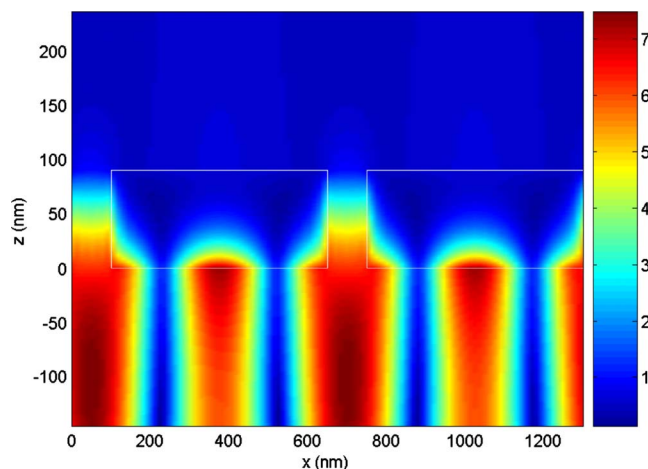
FIG. 4. (Color online) Amplitude of the magnetic field inside the structure and in its near field at the resonance wavelength. The grating is illuminated from below. The white rectangles shows the boundaries of the metallic grating.
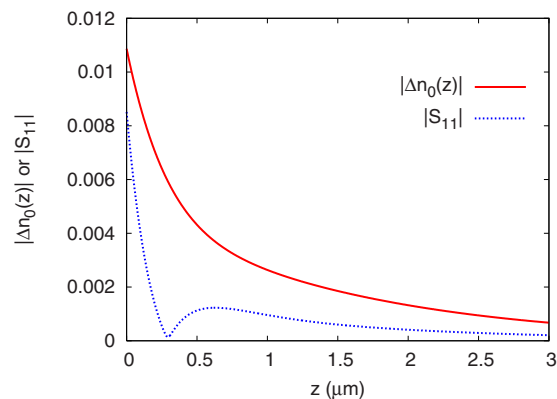

FIG. 5. (Color online) Modulus of the maximum amplitude of the elasto-optic modulation of the refractive index (solid line) and modulus of the longitudinal strain (dotted line) as a function of the distance to the interface. The SAW is propagating on Y-cut lithium niobate along the Z direction with a velocity of 3490 m/s and the frequency is 2.68 GHz. The acoustic aperture is set to 30 μm and the acoustic power to 1 W.

and is interacting with light incident on the nanostructured metallic film from the lithium niobate substrate side. In this section, we specifically consider that the SAW is generated by the metallic grating itself used as an IDT. As a consequence, the wavelength of the subsequent SAW is twice the period of the grating (the factor of 2 comes from the inter-digitation). As exposed in the Appendix, the displacement vector can be modeled for a SAW propagating along the x direction by

$$\mathbf{u}(x,z) = \mathrm{Re}\{\mathbf{u}_0(z)\exp[i(\omega t - kx)]\}, \tag{1}$$

where $\mathbf{u}_0(z)$ is the maximum amplitude of the displacement at height z and k is the wave vector. Inside a SAW resonator, a similar expression holds but the temporal and spatial dependencies separate. We assume that the metallic stripes do not significantly disturb SAW propagation from the free surface solution. For a SAW propagating on Y-cut lithium niobate along the Z direction, the velocity is 3490 m/s and the frequency is 2.68 GHz for $D=650$ nm. For definiteness, the acoustic aperture is set to 30 μm and the acoustic power to 1 W.

Four different acousto-optical effects are *a priori* expected: (i) modification of the refractive index of the substrate (and, to a much smaller extent, of the refractive index of the metal), as given by the elasto-optical effect; (ii) physical deformation of the surface in the vertical direction (z direction) due to the propagation of the acoustic wave, leading to the appearance of a "dynamic grating;" (iii) physical deformation of the grating in the longitudinal direction (x direction), which may change the period of the grating; and (iv) charge interaction between surface plasmons and the electric wave that propagates in the piezoelectric material along with the SAW. Effect (iv) is complex to quantify. It has been shown that acoustic waves can disturb conduction electrons (see, for instance, Ref. 22), but to the best of our knowledge, a direct interaction between a surface plasmon and an acoustic wave has never been reported. Indeed, there is a strong energy mismatch between an electromagnetic

wave like a surface plasmon and the SAW, making the interaction very weak. We will neglect it in the following. Effect (ii) (physical deformation of the film surface) was studied by Sun *et al.*[16] in the case of an unstructured silver film on LiNbO₃. They showed, in an attenuated total reflection setup, the effect of the acoustic dynamic grating on the plasmon resonance. However, this effect is pretty weak since the actual deformation of the surface of the film is less than 1 nm high, and hence we can neglect it. The SAW may also deform the grating in the x direction—effect (iii).[23] The SAW creates a longitudinal strain $S_{xx}=\partial u_x/\partial x$ that can affect the period of the grating D and the slit width d. The value of S_{xx} was computed via the theory developed in the Appendix [Eq. (A8)], see the corresponding plot of S_{xx} in Fig. 5, dotted line. From this computation, we estimate that the corresponding displacement u_x has a maximum value of roughly 5 nm for an IDT, exhibiting a period $D=650$ nm. Therefore, the period and slit width will experience variations up to 10 nm. Taking the parameters of Fig. 3, we have performed numerical computations with the Fourier modal method (not shown here). We have found that the longitudinal strain has only a weak influence on the transmission resonance: its spectral position is not affected and the transmission decreases of about 1%. Hence, in a first approximation, the longitudinal deformation of the grating may also be neglected. Keeping all these approximations in mind, we will focus our attention on the elasto-optical effect, that is to say, on the modification of the refractive index of the piezoelectric material (the elasto-optical effect in the metal can also be neglected due to the weak elasto-optic constants of gold).

Through the elasto-optical effect, the dielectric constant of the substrate (and also of the lithium niobate filling the slits) will be periodically modulated, roughly following the SAW wave form. Before running any electromagnetic calculation, the first step is therefore to estimate the elasto-optical variation of the refractive index of the substrate. The modulation of the refractive index can be modeled for a SAW propagating in the x direction by

$$\Delta n(x,z) = \text{Re}\{\Delta n_0(z)\exp[i(\omega t - kx)]\}, \qquad (2)$$

where $\Delta n_0(z)$ is the maximum amplitude of the modulation at height z. Principles of the computation of $\Delta n_0(z)$ are given in the Appendix. Figure 5 shows the modulus of $\Delta n_0(z)$ for a SAW propagating on Y-cut lithium niobate along the Z direction. It is clear from this figure that the maximum modulation is concentrated in the first micrometer below the surface of the substrate. From an electromagnetic point of view, the elasto-optic modulation can be modeled by layering dielectric gratings in the z direction. The value of the elasto-optic modulation inside the slits is set to the same value as the $z=0$ layer of the substrate.

The resulting transmission spectrum is not presented because it is indistinguishable from the undisturbed spectrum of Fig. 3. At first sight, this result could be attributed to the relatively low values of the acoustic perturbation of the refractive index. However, even if $\Delta n_0(z)$ is artificially increased by 1 order of magnitude, the transmission spectrum remains unaffected. Actually, the position of the transmission peak is governed by the spatial average value of the refractive index of the substrate. Since the SAW brings a periodic modulation which is null on average, no effect can be expected on the transmission spectrum.

Let us summarize the results of this section. We have first demonstrated that the mechanical deformations induced by the SAW are not strong enough to shift the transmission resonance. Hence, one has to rely only on the acousto-optic modulation of the refractive index. We also shown that this index variation should exhibit a non-null spatial average over a grating period. As a consequence, using the metallic grating exhibiting EOT as an interdigital transducer is an inefficient solution, and other interaction geometries must be looked for.

IV. MODULATION AND TUNABILITY OF THE EXTRAORDINARY TRANSMISSION

As shown in the previous section, the position of the resonance peak in the transmission spectrum is mainly governed by the average refractive index of the substrate. Consequently, to achieve EOT modulation, it is necessary to modulate globally the refractive index of the substrate. A simple way to do this is to use a high wavelength (i.e., low frequency) SAW. Since the diameter of the useful area of an actual nanostructured metallic film for EOT is rarely larger than a few tens of micrometers, a SAW with a wavelength of a few hundreds of micrometers will be large enough to globally affect the substrate. Such a SAW would be generated by an IDT separate from the nanostructured metallic grating exhibiting EOT. However, as noted earlier, the SAW will also induce a longitudinal strain that may deform the grating. Two configurations can be distinguished, depending on the polarization of the SAW.

(i) If the polarization of the SAW is parallel to the invariance axis of the EOT structure (y direction), then the physical deformation of the grating will not affect the geometrical parameters of the structure. Hence, the only relevant effect in this configuration will be the elasto-optical modulation of the refractive index of the substrate.

(ii) If the polarization of the SAW is not aligned with the invariance axis of the EOT structure, then a deformation of the grating will occur—the effect being maximum when the SAW polarization is perpendicular to the slits axis (x polarization). Strictly speaking, the deformation of the grating will break its periodicity, and an aperiodical numerical method (such as the finite-difference time-domain method) must be employed in order to perform a rigorous simulation of the optical properties of the deformed EOT structure. However, an estimate of the effect can be obtained if the deformation remains small with respect to the grating period. In this case, it may be taken into account by introducing an effective period $D_{\text{eff}}=D(1+S_{xx})$. Since the position of the transmission resonance is given by the product of the period times the substrate index (see Sec. II), and since Δn_0 and S_{xx} are of the same order of magnitude (see Fig. 5), one can infer that in the most favorable case, the total tuning range that is achievable in this configuration is twice the range obtained in configuration (i). Nevertheless, a more complete and rigorous study would be required since the two effects induced by the SAW may compete with each other. As a consequence, in the following, we restrict our study to the case where the SAW polarization is aligned with the direction of invariance of the slits and where the deformation of the EOT grating may be disregarded.

Keeping these assumptions in mind, we have performed numerical simulations of the transmission spectrum of the nanostructured metallic film (same parameters as in Sec. II) for different values of the substrate index. Note that the value of the refractive index inside the slits is set to the same value as the substrate. As shown on Fig. 6(a), the position of the resonance shifts with the refractive index. Moreover, the quality factor and the amplitude of the peak are not deteriorated. The position of the resonance is roughly given by $n_s \times D$, where n_s is the refractive index of the substrate. Therefore, the position of the transmission maximum follows a linear law, and an elasto-optic variation of the refractive index of $\Delta n=0.0015$ is necessary to shift the resonance by 1 nm. The amplitude of the shift can be further increased for higher values of the grating period, that is to say, for EOT at higher wavelengths. In terms of modulation, Fig. 6(a) shows the maximum displacement of the resonance, i.e., the spectrum when $\Delta n=\pm\Delta n_0$. In order to see the modulation effect, we have plotted on Fig. 6(b) the transmission efficiency versus time at two given wavelengths, taking for the temporal evolution of the elasto-optic modulation $\Delta n=\Delta n_0 \cos(\omega t)$. It appears that for $\Delta n_0=0.02$, a significant modulation of the transmission is observed. For $\lambda=1461.5$ nm (position of the resonance without the elasto-optic modulation), the transmission efficiency is modulated from about 61% at maximum to less than 10%. The rejection power is significantly improved if the wavelength is set to $\lambda=1474.5$ nm [red solid line in Fig. 6(b)]: in this case, the transmission drops to about 0.8% at $\omega t=\pi$.

Now let us focus our attention on the acoustic part of the problem: Is it possible to obtain such a Δn for low acoustic frequencies in a material such as LiNbO$_3$? Our calculations show that for classical IDTs, the value of the elasto-optic Δn tends to decrease at low frequencies. For instance, in Y-cut, Z-propagation lithium niobate at $f=50$ MHz (acoustic
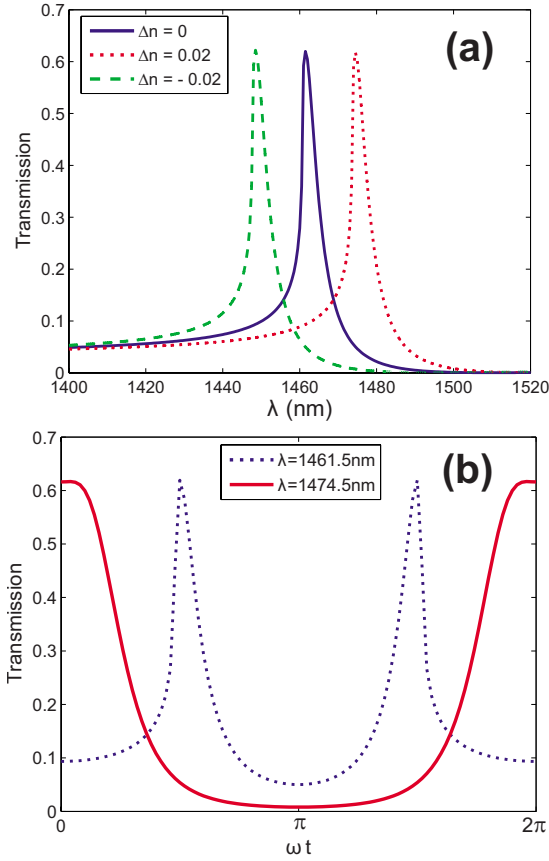
FIG. 6. (Color online) Modulation and tunability of the EOT by a low frequency SAW. (a) Transmission efficiency through the EOT structure for different values of the refractive index of LiNbO$_3$: no variation (solid line), $\Delta n = 0.02$ (dotted line), and $\Delta n = -0.02$ (dashed line). (b) Transmission efficiency vs time for a maximum modulation $\Delta n_0 = 0.02$ at $\lambda = 1461.5$ nm (dotted line) and $\lambda = 1447.5$ nm (solid line).

wavelength $= 70$ μm), we obtain $\Delta n = 2.6 \times 10^{-4}$ for an acoustic power of 1 W and an acoustic aperture of 1 mm. These values are not sufficient to obtain an useful tunability of the transmission peak. In order to achieve such an high elasto-optic interaction, it will be necessary to use more efficient acoustic transducers to concentrate the acoustic energy. For instance, annular acoustic transducers can be designed to resonantly focus the acoustical power at their center.[24] If an EOT grating is located at the center of such a device, it would experience a strong acoustic field, sufficient to achieve optical tunability and modulation with a reasonably good bandwidth.

V. CONCLUSION

We have reported on the optical properties of an EOT structure deposited onto the top of a piezoelectric material. A simple structure presenting a high amplitude transmission resonance has been proposed. This resonance is linked to the excitation of a surface plasmon along the substrate/metal interface, and its spectral position can be tuned by changing the substrate refractive index. A long wavelength SAW could

be used to obtain this global change of refractive index. A good tunability is observed, providing that the index variation is high enough. This shows that acoustic waves are an interesting route for the realization of controllable EOT devices and, more generally, of active plasmonic devices. The main difficulty in the actual realization of such structures is to obtain sufficiently high values of Δn. Acoustic resonators could be a elegant way to concentrate acoustic power on an EOT device in order to reach an useful tunability range. Such resonators are currently under investigation in our group.

APPENDIX: REFRACTIVE INDEX VARIATION INDUCED BY A RAYLEIGH SURFACE WAVE

In this appendix, we derive the computation of the refractive index variation induced by a Rayleigh surface wave propagating atop a piezoelectric semi-infinite medium. The formulation we use for expressing Rayleigh surface acoustic waves is based the traditional expansion over partial waves approach, for instance, given in Ref. 25. The displacements inside the piezoelectric medium are expressed as a superposition on partial waves according to

$$u_i = \sum_{j=1}^{4} U_{ij} a_j \exp\{\imath\omega[t - s_1 x_1 - s_2(j)x_2]\}, \tag{A1}$$

where x_1 is the coordinate in the propagation direction and x_2 is the depth coordinate. ω is the angular frequency, s_1 is the Rayleigh wave slowness (the inverse of the phase velocity), U_{ij} is a 4×4 square matrix gathering the displacements of the partial waves, and $s_2(j)$ is the slowness component is the depth of the jth partial wave. The a_j are modal amplitudes that are determined from the boundary conditions. Both indices i and j run from 1 to 4. The fields are assumed to be independent of the x_3 coordinate. A similar expression is used to express the stress tensor as

$$T_{ki} = \sum_{j=1}^{4} T_{ij}^{(k)} a_j \exp\{\imath\omega[t - s_1 x_1 - s_2(j)x_2]\}, \tag{A2}$$

where the index k runs from 1 to 3. In the domain of existence of Rayleigh surface waves, $s_2(j)$ are complex with a negative imaginary part. It should be noted that they are obtained as the eigenvalues of a generalized eigenvalue problem, the eigenvectors of which also yields the matrices U_{ij} and $T_{ij}^{(k)}$. The free surface or the shorted surface boundary conditions are used here. The Rayleigh wave slowness is then obtained by searching for a zero of the boundary condition determinant as a function of s_1. This condition determines both s_1 and the partial waves amplitudes a_j up to a multiplicative factor.

The acoustic energy distribution in the depth is treated as follows. The acoustic intensity transported by each partial

wave is integrated on a semi-infinite surface orthogonal to the propagation direction to give

$$I(j) = \frac{w|a_j|^2 P_1(j)}{2\omega\alpha_2(j)}, \tag{A3}$$

where w is the acoustic aperture, $\alpha_2(j) = -\text{Im}\{s_2(j)\}$, and

$$P_1(j) = \text{Re}\left(-\iota\omega\sum_{n=1}^{4} U_{nj}^* T_{nj}^{(1)}\right) \tag{A4}$$

is the component of the Poynting vector the jth partial wave directed along the propagation direction. By imposing a given acoustic intensity of the beam I expressed in watts, the energetic distribution over the four partial waves can be obtained via the normalization relation

$$I = I(1) + I(2) + I(3) + I(4). \tag{A5}$$

As said above, the partial waves amplitudes a_j are only determined up to a multiplicative factor by the boundary conditions, i.e., we write $a_j = a a_j'$ where the a_j' are the known unnormalized values. Inserting Eq. (A4) in Eq. (A5) yields

$$I = \frac{a^2 w}{2\omega}\sum_{j=1}^{4} \frac{P_1(j)}{\alpha_2(j)}|a_j'|^2. \tag{A6}$$

This equation determines a and then the correctly normalized a_j values.

The strain tensor is next derived from Eq. (A1) according to its definition,

$$S_{ij} = \frac{1}{2}\left(\frac{\partial u_i}{\partial x_j} + \frac{\partial u_j}{\partial x_i}\right). \tag{A7}$$

This symmetric tensor reads

$$S_{11} = -\iota\omega s_1 U_{1j}\exp[-\iota\omega s_2(j)x_2]a_j, \tag{A8}$$

$$S_{22} = -\iota\omega s_2(j)U_{2j}\exp[-\iota\omega s_2(j)x_2]a_j, \tag{A9}$$

$$S_{33} = 0, \tag{A10}$$

$$S_{23} = -\iota\omega s_2(j)U_{3j}\exp[-\iota\omega s_2(j)x_2]a_j, \tag{A11}$$

$$S_{13} = -\iota\omega s_1 U_{3j}\exp[-\iota\omega s_2(j)x_2]a_j, \tag{A12}$$

$$S_{12} = -\iota\omega s_2(j)U_{1j}\exp[-\iota\omega s_2(j)x_2]a_j$$
$$-\iota\omega s_1 U_{2j}\exp[-\iota\omega s_2(j)x_2]a_j. \tag{A13}$$

The elasto-optic tensor is then used to obtain the variation of the optical impermittivity tensor as

$$\Delta\eta_{ij} = p_{ijkl}S_{kl}, \tag{A14}$$

which translates in the optical dielectric permittivity tensor through

$$\Delta\epsilon_{ij} = -\epsilon_{ik}\Delta\eta_{kl}\epsilon_{lj}. \tag{A15}$$

This last quantity allows one for the computation of the refractive index variation with

$$\Delta n = \frac{d_i^{(1)}\Delta\epsilon_{ij}d_j^{(2)}}{2\sqrt{d_i^{(1)}\epsilon_{ij}d_j^{(2)}}}, \tag{A16}$$

where $d_i^{(1)}$ and $d_i^{(2)}$ are the components of the unit vectors defining the input and output optical polarizations, respectively.

---

*Present address: Institut Fresnel, Domaine Universitaire de Saint Jérôme, F-13397 Marseille Cedex 20, France.

[1] T. W. Ebbesen, H. J. Lezec, H. F. Ghaemi, T. Thio, and P. A. Wolff, Nature (London) **391**, 667 (1998).

[2] J. A. Porto, F. J. Garcia-Vidal, and J. B. Pendry, Phys. Rev. Lett. **83**, 2845 (1999).

[3] H. J. Lezec, A. Degiron, E. Devaux, R. A. Linke, L. Martin-Moreno, F. J. Garcia-Vidal, and T. W. Ebbesen, Science **297**, 820 (1998).

[4] D. Gérard, L. Salomon, F. de Fornel, and A. V. Zayats, Phys. Rev. B **69**, 113405 (2004).

[5] D. Van Labeke, D. Gérard, B. Guizal, and F. I. Baida, Opt. Express **14**, 11945 (2006).

[6] J. A. H. van Nieuwstadt, M. Sandtke, R. H. Harmsen, F. B. Segerink, J. C. Prangsma, S. Enoch, and L. Kuipers, Phys. Rev. Lett. **97**, 146102 (2006).

[7] A. Lesuffleur, L. Kiran Swaroop Kumar, and R. Gordon, Appl. Phys. Lett. **88**, 261104 (2006).

[8] H. Rigneault, J. Capoulade, J. Dintinger, J. Wenger, N. Bonod, E. Popov, T. W. Ebbesen, and P.-F. Lenne, Phys. Rev. Lett. **95**, 117401 (2005).

[9] A. Lesuffleur, H. Im, N. C. Lindquist, and S.-H. Oh, Appl. Phys. Lett. **90**, 243110 (2007).

[10] F. I. Baida, Y. Poujet, B. Guizal, and D. Van Labeke, Opt. Commun. **256**, 190 (2005).

[11] A. V. Zayats, I. I. Smolyaninov, and A. A. Maradudin, Phys. Rep. **408**, 131 (2005).

[12] C. Genet and T. W. Ebbesen, Nature (London) **445**, 39 (2007).

[13] I. I. Smolyaninov, A. V. Zayats, A. Stanishevsky, and C. C. Davis, Phys. Rev. B **66**, 205414 (2002).

[14] *Handbook of Optical Constants of Solids*, editor E. D. Palik (Academic, New York, 1985).

[15] W. C. Chew, *Waves and Fields in Inhomogeneous Media* (IEEE, New York, 1995).

[16] X. Sun, S. Shiokawa, and Y. Matsui, J. Appl. Phys. **69**, 362 (1991).

[17] L. Li, J. Opt. Soc. Am. A **20**, 655 (2003).

[18] G. Granet and B. Guizal, J. Opt. Soc. Am. A **13**, 1019 (1996).

[19] L. Li, J. Opt. Soc. Am. A **13**, 1870 (1996).

[20] F. I. Baida and D. Van Labeke, Opt. Commun. **209**, 17 (2002).

[21] S. Collin, F. Pardo, R. Tessier, and J.-L. Pelouard, J. Opt. A, Pure Appl. Opt. **4**, 154 (2002).

[22] M. Rotter, A. V. Kalameitsev, A. O. Govorov, W. Ruile, and A. Wixforth, Phys. Rev. Lett. **82**, 2171 (1999).

[23] M. M. de Lima Jr., R. Hey, P. V. Santos, and A. Cantarero, Phys. Rev. Lett. **94**, 126805 (2005).

[24] C. K. Day and G. G. Koerber, IEEE Trans. Sonics Ultrason. **SU-19**, 461 (1972).

[25] V. Laude, M. Wilm, and S. Ballandras, J. Appl. Phys. **93**, 10084 (2003).